

Scientific paper

Melt Spinning of Plastic-Grade Polypropylene

Diana Gregor-Sveteč

University of Ljubljana, Faculty of Natural Sciences and Engineering, Snežniška 5,
SI-1000, Ljubljana, Slovenia

* Corresponding author: E-mail: diana.gregor@ntf.uni-lj.si

Received: 05-02-2009

Abstract

The goals of our research were to optimize the melt spinning of filaments spun from plastic-grade polypropylene polymer and to compare the structural characteristics of as-spun filaments obtained from plastic- and fiber-grade polymers. The melt spinning of polypropylene filaments was carried out on an Extrusion Systems Ltd. laboratory spin-draw device. The spinning process was optimized in order to avoid the onset of spinline instabilities and spinline diameter fluctuations and was carried out as gravitational spinning with no-take-up application. From measurement of the average molecular weight and molecular weight distribution, some degradation of molecules and narrowing of molecular weight distribution in both types of as-spun filaments was determined. At both tested as-spun filaments, produced by rapid cooling of an extruded jet, only the spherulitic structure composed of α -monoclinic crystals was established. In comparison to the filaments spun from the fiber-grade polymer, filaments spun from the plastic-grade polymer had higher density, melting enthalpy, and higher crystallinity, resulting in higher tenacity of these filaments.

Keywords: Polypropylene, melt spinning, as-spun filaments, WAXS, SEM, SEC/LALLS

1. Introduction

Mechanical performance of semicrystalline filaments is determined by the filament molecular characteristics, which are mainly affected by processing conditions; although the polymer molecular structure also has some influence on them. Many studies have dealt with the development of morphology during extrusion and uniaxial stretching of polypropylene films and filaments. By changing the processing conditions and molecular parameters, a wide range of molecular structures can be produced, such as spherulites, shish-kebab, row-nucleated, and paracrystalline structures. It was reported^{1–3} that under quiescent conditions, a spherulitic structure with no globally preferred orientation is formed. If isotactic polypropylene is solidified under the action of stress, it forms a more complex, cylindrical, row-nucleated structure with some state of orientation.^{4,5} In some studies, it was reported that rapid cooling leads to a mesomorphic so-called smectic structure, while moderate to high speeds in spinline results in filaments exhibiting a monoclinic structure.^{6–8}

Andreassen et al.⁹ have reported that in all filaments with broad molecular weight distribution, a monoclinic α phase with bimodal orientation was found, while in filaments with narrow molecular weight distribution, a unia-

axially oriented mesomorphic phase was obtained. Previous research^{10–12} has shown that the crystallinity degree and crystallization rate is increased by lowering the molecular weight of the polymer and that the crystallization speed increases with the broader molecular weight distribution. Misra et al.¹³ found that the degree of crystallinity increases with the take-up velocity, particularly in polymers with a narrow molecular weight distribution, while polymers with broader distribution reached a high level of crystallinity at lower speeds.

Han^{14,15} suggested that similar flow properties are attained when films and/or fibers are extruded at equivalent shear rates and comparable extrusion velocities. Janarthanan et al.¹⁶ reported that films and fibers prepared under similar conditions would produce similar morphologies. In our study, polypropylene filaments were spun under similar conditions from two polymers of different molecular weight and molecular weight distribution. Filaments were extruded at the same melt output rate and extrusion speed, and with identical quenching conditions in the process of gravitational spinning with no-take-up application. The aim of the study was determination of the structural characteristics and tensile properties of as-spun filaments and evaluation of the influence of molecular weight and molecular weight distribution of polymers on the structure of filaments.

2. Experimental

2. 1. Sample Preparation

As-spun filaments were made from Ziegler-Natta catalyzed polypropylene chips, a plastic grade homopolymer with a melt flow index (MFI) is 2 g/10 min and a fiber-grade homopolymer with a MFI is 18 g/10 min. The MFI was determined as the amount of polymer extruded at a temperature of 230 °C, with a forcing load of 2160 g over 10 min. A plastic-grade polymer is a broad molecular weight distribution polymer, with the ratio of weight average to number average molecular weight of $M_w/M_n = 5$, while a fiber-grade polymer is a narrow molecular weight distribution polymer, a so-called controlled rheology or CR-polymer, with $M_w/M_n = 3.3$. The melt spinning of PP filaments was carried out on an Extrusion Systems Ltd. laboratory spin-draw device. The filaments were extruded through a spinneret with ten holes each of diameter 0.35 mm. The temperature of the melt at the spinneret was set at 235 °C for the fiber-grade polymer and at 285 °C for the plastic-grade polymer. The set melt pressure in the extruder was the same for both polymers, 4.8 MPa. Also the melt output rate (mass flow rate) of 21.7 g/min was the same for both polymers. Cooling of the resultant filaments was achieved with cross-flow air quenching at an air temperature of 2 °C.

2. 2. Characterization

Wide-angle x-ray scattering (WAXS) and small-angle x-ray scattering (SAXS) techniques were used to explore the structure of drawn PP fibers. Copper radiation was monochromatized by means of a 10 μm Ni filter. WAXS and SAXS film patterns were taken on a vacuum flat-film camera with pinhole collimation. WAXS curves (intensity as a function of scattering angle (2θ)) were made for normal transmission geometry of samples by using a two-circle goniometer developed by Kratky. The scattered intensities were registered with a Braun PSD 50M position-sensitive detector in the angular range from $2\theta = 9.5^\circ$ to 31.5° , for each azimuthal position of the fiber axis from $\phi = 0^\circ$ to 180° . The intensities obtained were corrected for polarization, absorption, background, and incoherent scattering. The degree of crystallinity was estimated by the Hermans and Weidinger method over the angular range from $2\theta = 10$ to 30. The apparent crystallite dimensions were determined by means of the Scherrer's equation from the experimental reflection profiles corrected for instrumental broadening.

The crystalline fraction in the fibers was also evaluated from density data and DSC-thermograms. The density of drawn fibers was determined with the flotation method, as described by Juilfs, using a mixture of isopropylalcohol and water. The melting behavior of the samples in the temperature range from 40 °C to 200 °C was examined at a constant heating rate of 10 °C/min with a Perkin-Elmer DSC-7 calorimeter.

Morphological studies were conducted using scanning electron microscopy of the filament surface. Filaments were also etched in a chromic acid solution at room temperature. A JEOL JSM-2 electron microscope was used for all morphological studies.

Molecular weights were determined with a SEC/LALLS system containing a Model L-510 pump (Waters), Model 7010 injector (Rheodyne) columns TSK GMH6-HT (Toyo Soda Manufacturing Co.Ltd.), LiCrogel PS40000 and PS4 (Merck) columns, equipped with a KMX-6 low-angle laser light scattering photometer (Chromatix, Inc.) and an infrared detector (DuPont Industries Company). The experiments were run with a flow rate of 1 ml/min at 135 °C and the nominal injection volume was 305 μL . A LALLS photometer with a high-temperature flow-through cell was connected with the column. Scattering intensity data were collected using a 6–7 degree forward-scattering annulus with a 633 nm wavelength He-Ne laser. Polymer concentration in the eluent was monitored with an infrared detector, and a 3.41 μm narrow bandpass filter was also used. All solutions for analysis were prepared in filtered 1,2,4-trichlorobenzene (TCB), the same solvent used as the SEC eluent. Polymer solutions were prepared by dissolving known quantities of polypropylene and diluting to the desired volume with the filtered TCB solvent. Dissolution of PP samples was achieved by rotating the samples at 160 °C for 24 h. An antioxidant was added to prevent oxidative degradation of PP. The SEC column was calibrated using polystyrene standard samples.

The tensile properties of as-spun filaments were measured with an Instron 6022 tensile testing machine. Filaments were tested with a gauge length of 20 mm and an extension rate of 20 mm/min. Test were carried out 20 times for each sample.

3. Results and Discussion

Multifilament yarns composed from ten filaments were spun from two different polypropylene homopolymers, a polymer in the medium molecular weight range used for textile applications (fiber-grade polymer), and a polymer with a higher molecular weight used in the technical sector (plastic-grade polymer). Free-running filaments were collected at the exit of the cooling chamber just before the feed roll (godet), and formed without tension caused by the winding on a take-up device, to avoid stress-induced crystallization and resulting orientation.

Comparison of the linear density of both samples of undrawn filaments confirmed the differences in the rheological and spinning properties of both polymers. The linear density of multifilament yarn spun from the plastic-grade polymer, i.e., higher molecular weight polymer of broader molecular weight distribution (sample 1), was

659 tex. For the multifilament yarn spun from the fiber-grade polymer, i.e., lower molecular weight CR-polymer (sample 2), the linear density was 488 tex. The mean diameter of the single filament determined from sample 1 was 97 μm , and for sample 2 it was 84 μm . Despite the same spinneret orifice diameter (0.35 mm), the same mass flow rate (21.7 g/min), temperature, and cooling rate of air in the cooling chamber, the differences in the temperature of the melt and molecular structure of the polymer resulted in different flow intensity, elongational viscosity, and, consequently, different diameters for the solidified filaments. These differences resulted in variations in the level of stress in the spinline and also in differences in the structure of filaments. Nadela et al.¹⁷ and Lu and Spruiell¹⁸ have shown that the molecular weight and molecular weight distribution have major effects on the development of structure during melt spinning of polypropylene. Higher elongational viscosity associated with higher weight average molecular weight produces a more rapid buildup of stress in the spinline, which results in a more rapid buildup of orientation and crystalline order.

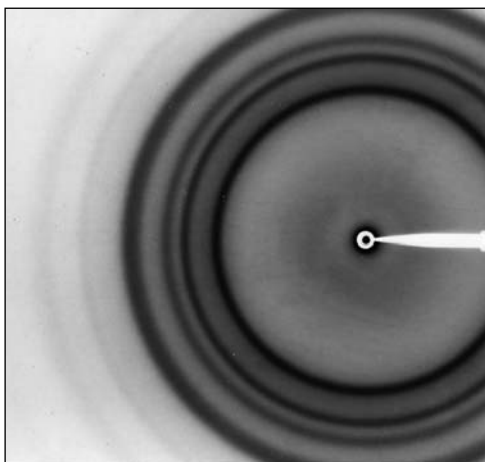
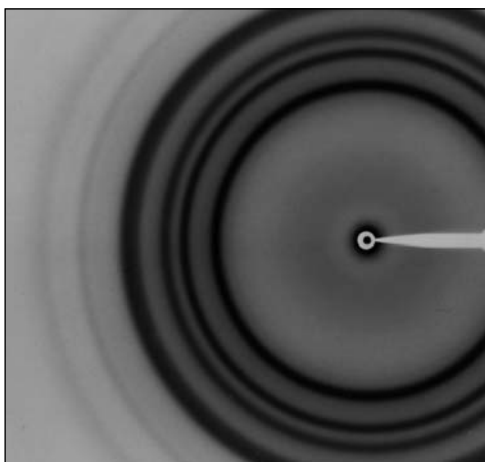


Figure 1. WAXS film pattern (fiber axis vertical) of as-spun filaments made from the plastic-grade polymer (a) and the fiber-grade polymer (b).

The WAXS film patterns obtained for both as-spun multifilament yarns (Fig. 1) show continuous Debye-Scherrer rings on the film, meaning that an unoriented structure is present in the filaments. The intense reflection rings of planes (110), (040), (130), (111), ($\bar{1}$ 31) (041) are visible. This means that the structure is isotropic and consists of spherulites composed of α -monoclinic crystals, which are oriented in different directions. On the SAXS pattern, a diffuse equatorial scattering in the form of a continuous ring is seen, confirming the presence of unoriented or spherically oriented bundles of crystallites (Fig. 2). The same SAXS pattern was obtained at both samples.

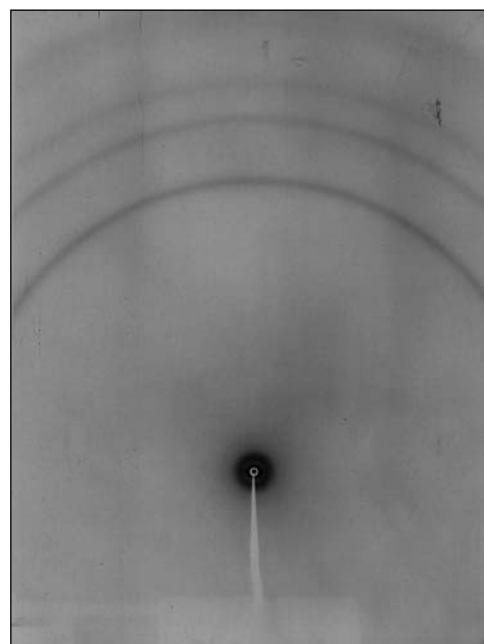


Figure 2. SAXS film pattern (fiber axis vertical) of as-spun filaments made from the plastic-grade polymer.

Apparent crystallite dimensions were determined by means of Scherrer's equation¹⁹ from the half-widths of diffraction curves of crystalline peaks which were approximated by pseudo-Voigt functions.

$$L_{hkl} = \frac{K\lambda}{\beta_0 \cos \theta}, \quad (1)$$

In equation 1 L_{hkl} is the mean size of the crystallites perpendicular to the planes (hkl), β_0 is the breadth of the reflection profile (in radians) at half-maximum intensity, and K is a constant that is assigned a value of 0.9 for PP. The crystals and noncrystalline regions are organized into supramolecular structures – spherulites in the as-spun filaments. Here, the crystalline regions are composed of individual crystallites, which are formed from molecules folded back on themselves. Crystallites in filaments have

quite large dimensions, a little larger in the filaments spun from the plastic-grade polymer as seen from Fig. 3. The apparent crystallite dimensions in the direction perpendicular to the fiber axis, as determined from equatorial reflections (110), (040) and (130), are larger than the cross dimension of crystallites in the direction [hkl].

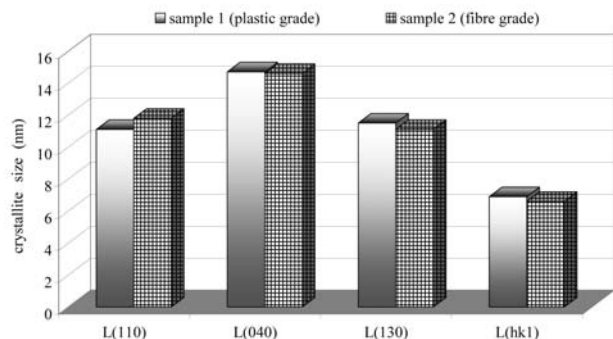


Figure 3. Apparent crystallite dimension perpendicular to the plane (hkl) of as-spun filaments made from the plastic-grade polymer (sample 1) and the fiber-grade polymer (sample 2).

The WAXS diffractograms are shown in Fig. 4. The degree of crystallinity was evaluated from the WAXS diffraction curves over the angular range from $2\theta = 10$ to 30 by resolving multiple peak data into individual crystalline peaks and an amorphous halo. In accordance with Hermans-Weidinger's method²⁰, the crystallinity was calculated as the ratio of the integrated scattering under the resolved crystalline peaks to the total scattering of the sample. The content of crystalline regions in the both as-spun multifilament yarns is low, about 25% higher in filaments spun from the plastic grade polymer.

The crystalline fraction in filaments was also evaluated from density data and DSC-thermograms. The density of PP multifilament yarns was determined with the flotation method, using a mixture of isopropylalcohol and water. The crystallinities of the samples were then calcu-

lated by the equation

$$x_{DENSITY} = \frac{\rho_c(\rho - \rho_{am})}{\rho(\rho_c - \rho_{am})} 100\% \quad (2)$$

where ρ is the sample density, and ρ_c ($\rho_c = 0.9380$) and ρ_{am} ($\rho_{am} = 0.8545$) are the densities of the crystalline and amorphous phases, respectively.

From the measured melting enthalpy (ΔH), the crystallinity was derived from the following equation

$$x_{DSC} = \frac{\Delta H}{\Delta H_c} \cdot 100\%, \quad (3)$$

where ΔH_c is the melting enthalpy of 100% crystalline PP and was assumed in this work at 209 J/g.

Higher density, with a value of 0.8934 g/cm³ and a 20% higher degree of crystallinity, was determined in filaments spun from the plastic-grade polymer (sample 1). Also, crystallinity evaluated from the DSC-thermograms was higher in sample 1 (Fig. 5).

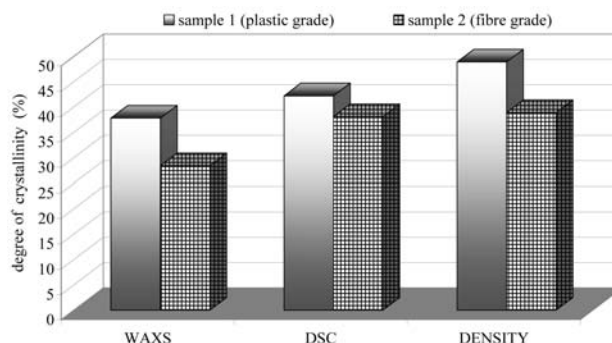


Figure 5. Degree of crystallinity evaluated from WAXS curves, DSC thermograms, and density data of as-spun filaments made from the plastic-grade polymer (sample 1) and the fiber-grade polymer (sample 2).

As shown from the DSC-thermograms, the melting range is broader in as-spun filaments made from the pla-

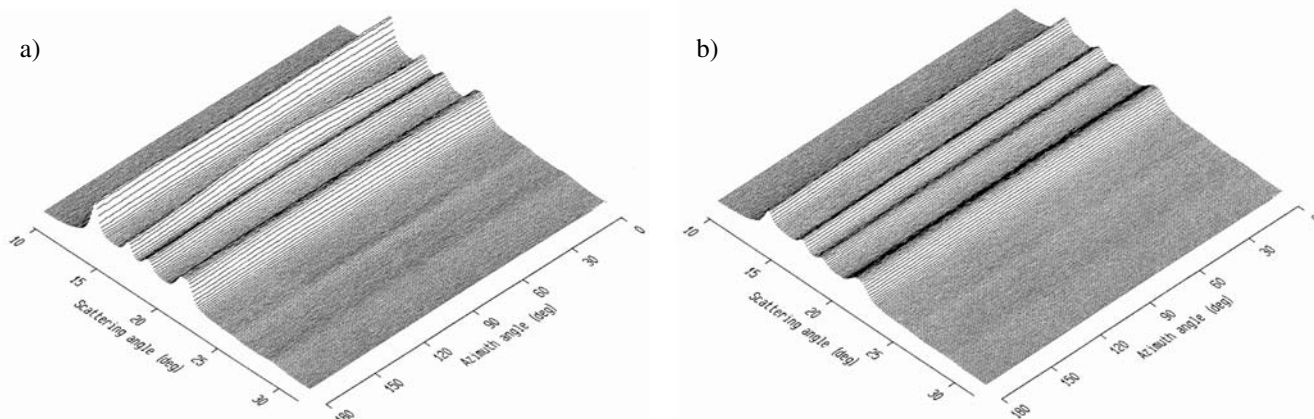


Figure 4. WAXS intensity maps of as-spun filaments made from the plastic-grade polymer (a) and the fiber-grade polymer (b).

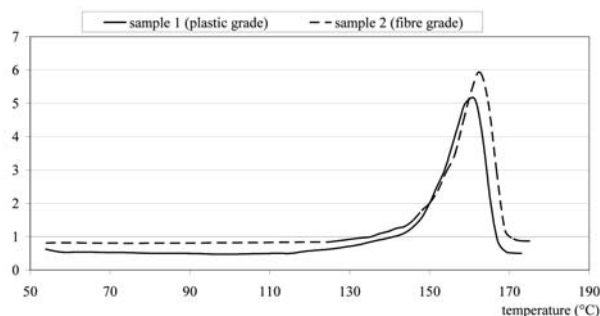


Figure 6. DSC thermograms of as-spun filaments made from the plastic-grade polymer (sample 1) and the fiber-grade polymer (sample 2).

stic-grade polymer. These filaments began to melt at 115 °C and had a maximum melting temperature of 160.7 °C. In contrast, the as-spun filaments made from the fiber-grade polymer started to melt at 132 °C and the maximum melting occurred at 162.7 °C. A broader peak in the as-spun filaments made from the plastic-grade polymer resulted in higher melting enthalpy of this sample, as seen from Table 1.

As-spun filaments made from the fiber-grade polymer have a smooth surface (Fig. 7b), whereas the filaments made from the plastic-grade polymer (Fig. 7a) show some surface features, and the surface is generally rougher. This can be a consequence of inline instabilities

Table 1. Density (ρ), onset temperature of the melting peak (T_{start}), end temperature of the melting peak (T_{end}), maximum temperature of the melting peak (T_m), melting enthalpy (ΔH) of as-spun filaments made from the plastic-grade polymer (sample 1) and the fiber-grade polymer (sample 2).

Sample	ρ (g/cm ³)	T_{start} (°C)	T_{end} (°C)	T_m (°C)	ΔH (J/g)
Sample 1 (plastic grade)	0.8934	115.1	169.5	160.7	88.1
Sample 2 (fiber grade)	0.8851	132.0	173.5	162.7	79.5

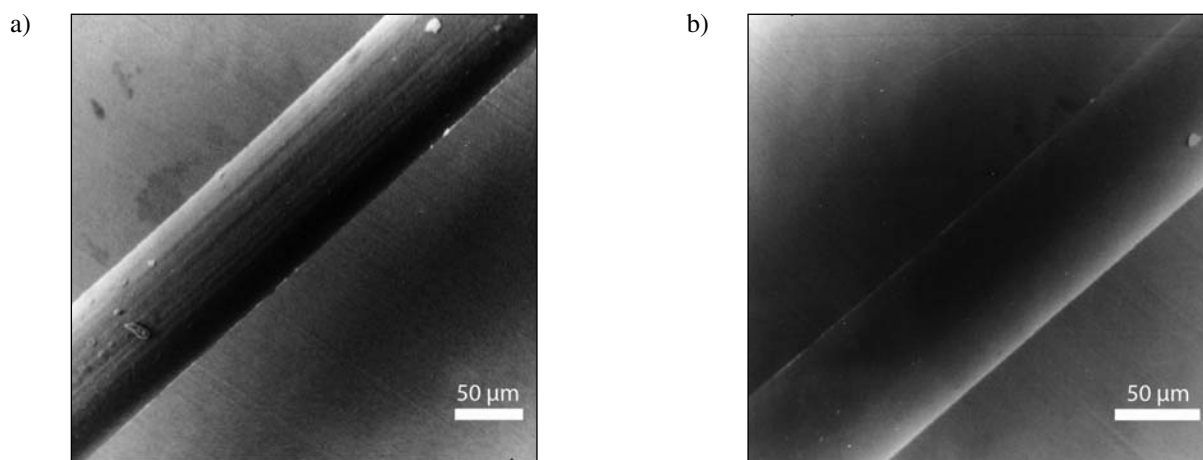


Figure 7. SEM micrographs of as-spun filaments made from the plastic-grade polymer (a) and the fiber-grade polymer (b).

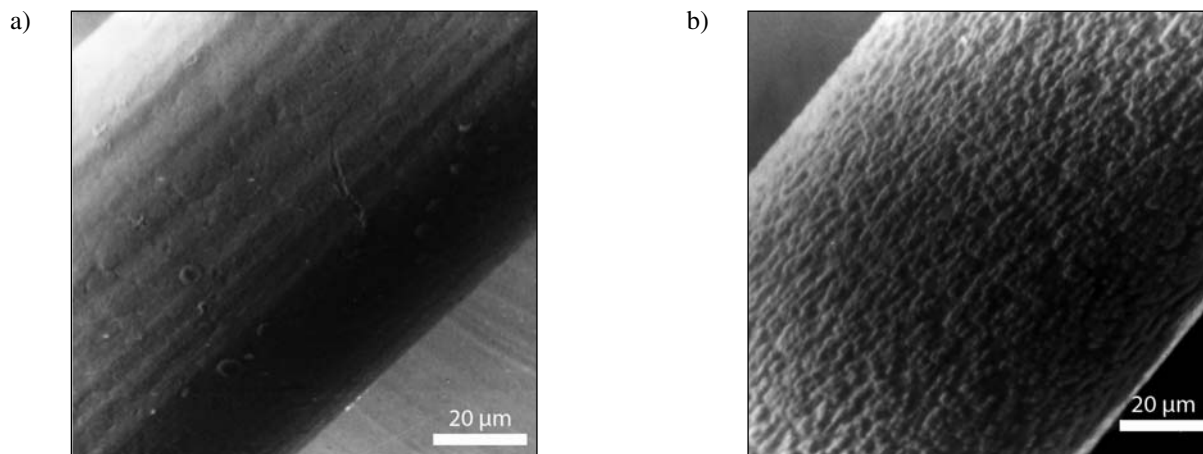


Figure 8. SEM micrographs before (a) and after 48-hour etching (b) of as-spun filaments made from the plastic-grade polymer.

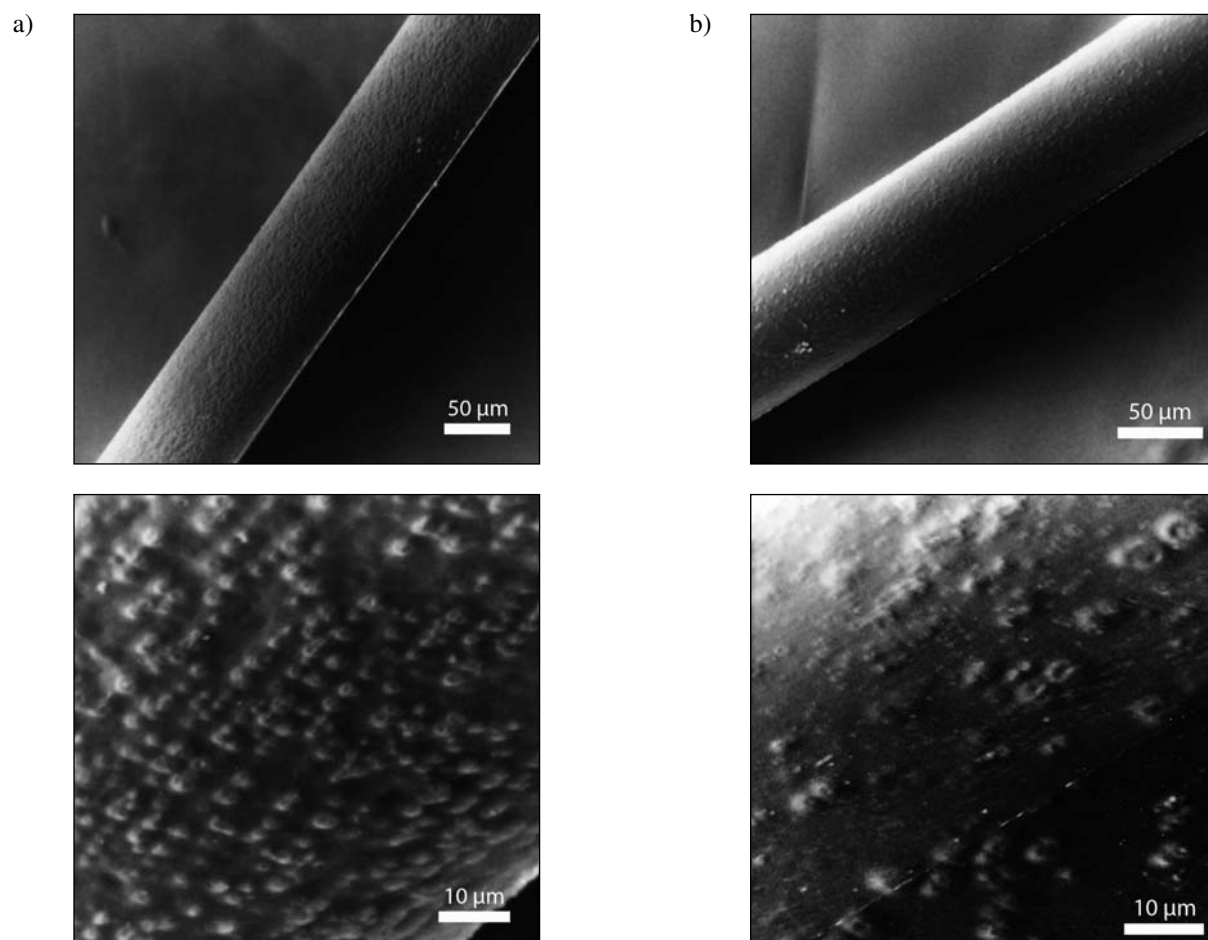


Figure 9. SEM micrographs after 48-hour etching of as-spun filaments made from the plastic grade-polymer (a) and the fiber-grade polymer (b).

which appear in spinning of highly viscous polymers and slower cooling of extruded filaments. Etching in chromic acid caused dissolving of noncrystalline areas between spherulites on the surface of the filaments. This can be observed from the SEM micrographs, which show that the smooth filament's surface before etching (Fig. 8a) became grainy (Fig. 8b). These grainy protrusions are spherulites, which are less soluble because of their more ordered partly crystalline structure. The frequency of these grains is higher in the filaments spun from the plastic-grade polymer (Fig. 9a) than in filaments spun from the fiber-grade polymer (Fig. 9b). The density and melting enthalpy demonstrate that these filaments are more crystalline and may also have a more stable crystalline structure than filaments spun from the fiber-grade polymer. The higher average molecular weight of filaments spun from the plastic-grade polymer and the longer macromolecules present ($\overline{M}_z = 788,600$ and M10% high molecular fraction = 1,166,430), compared with these values obtained in filaments spun from the fiber-grade polymer (Table 2), enables the formation of crystallizing nuclei at a higher temperature and in shorter time, which at a higher temperature of extruded jet and solidified filaments leads to a higher

level of crystallinity and most likely smaller spherulites; this can be concluded from the smaller grains seen in SEM images of etched filaments.

The average molecular weights were measured by size exclusion chromatography with low-angle laser light-scattering detection (SEC/LALLS). The molecular weight is given by following equation (Eq. 4):

$$\overline{M} = \frac{\sum c_i M_i^j}{\sum c_i M_i^{j-1}} \quad (4)$$

where $j = 0$ gives the number average molecular weight (\overline{M}_n), $j = 1$ gives weight average molecular weight (\overline{M}_w), and $j = 2$ gives Z average, the average molecular weight of longer molecules (\overline{M}_z). As M_i values were determined by light scattering, they are weight average values for the solute mixture eluted at the given time and are determined at uniform intervals on the elution curve. The concentration c_i may be calculated directly from the amplitude x_i of the concentration detector, or the detector response can be normalized as follows:

$$c_i = \frac{m \cdot x_i}{V_i \cdot \sum x_i} \quad (5)$$

where m is the mass injected, V_i is the effluent volume passing through the sample cell during the i -th interval, and $\sum x_i$ is the sum of the x_i values for all intervals within the peak.

The sample intrinsic viscosity is determined with the following equation:

$$[\eta] = \frac{\sum(\eta_{spi} \delta V_i)}{m} \quad (6)$$

The summation term in Eq. 6 is the area under the eluted sample peak within the specific viscosity chromatogram envelope measured by the concentration detector, and m is the total mass of polymer injected.

Number average molecular weight and weight average molecular weight were determined from the data obtained with the concentration detector and with the LALLS signal. The comparison of these values determined with two different evaluation methods at both samples yielded a good match. The determined values are given in Table 2.

Table 2. SEC results: number average molecular weight (\bar{M}_n), weight average molecular weight (\bar{M}_w), Z average, average molecular weight of longer molecules (\bar{M}_z), viscosimetric molecular weight (\bar{M}_v), $\bar{M}_{10\%}$ molecular weight of low molecular fractions and high molecular fractions, intrinsic viscosity ($[\eta]$) and polydispersity index (I_p) of as-spun filaments made from the plastic-grade polymer (sample 1) and the fiber-grade polymer (sample 2).

	Sample 1 (plastic grade)	Sample 2 (fibre grade)
\bar{M}_n (g/mol)	60400	75600
\bar{M}_w (g/mol)	273300	201400
\bar{M}_z (g/mol)	788600	449400
\bar{M}_v (g/mol)	227800	177800
$\bar{M}_{10\%}$ low molecular fractions (g/mol)	15530	22200
$\bar{M}_{10\%}$ high molecular fractions (g/mol)	1166430	704940
$[\eta]$ (dL/g)	1.45	1.22
I_p (I)	4.5	2.7

Filaments spun from the plastic-grade polymer have a higher weight average and viscosimetric molecular weight and a lower number average molecular weight than filaments spun from the fiber-grade polymer. The higher number average molecular weight of this sample is expected because number molecular weight is mainly influenced by the shorter molecules, and filaments spun from the fiber-grade CR-polymer have a higher share of low molecular weight fractions. Also, the lower weight average and viscosimetric molecular weight at these filaments is expected, since the very long molecules are not present in CR-polymers. The difference between both samples is very large at average molecular weight of longer molecules and at the 10% of high molecular weight fractions.

Comparison of the number average and weight average molecular weight of the raw material (polymer chips) and as-spun filaments has revealed that after spinning, the number average molecular weight was slightly increased,

while weight average molecular weight slightly decreased in both as-spun filaments. Because of this, the polydispersity index, which is the measure of the molecular weight distribution, is slightly smaller at both as-spun multifilament yarns, meaning that the distribution of molecular weights is narrower. This means that during spinning, some scission of molecular chains occurred because of high spinning temperature leading to thermal degradation.

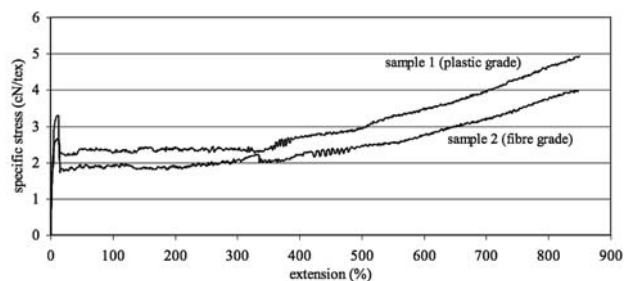


Figure 10. Specific stress vs. extension curve of as-spun filaments made from the plastic-grade polymer (sample 1) and the fiber-grade polymer (sample 2).

Mechanical properties of both of the as-spun multifilament yarns are similar; they break at an extension of 850%, and low specific stress of 4.9 cN/tex for filaments spun from the plastic grade polymer and 4 cN/tex at filaments spun from the fibre grade polymer. The specific stress-extension curves of both as-spun multifilament yarns have a typical shape for the unoriented partly-crystalline polymeric material: a steeply rising first part, a distinguished turning point, a drop in specific stress after the turning point with an ongoing straight part, and a more rapid incline before the break. These four distinct regions are: elastic, yield, drawing with neck, and the postneck region. The yield point can be represented as the point at which shear forces within the spherulites predominate, leading to lamellar slip. The drop from the higher stress to lower stress at yield is a consequence of strain softening of the spherulitic structure. As strain continues beyond the yield point, the spherulites are drawn out but preserve

their continuity intraspherulitically. Deformation of the spherulites continues by the processes of lamellar slip, orientation, and separation, until the lamellae in all regions of the spherulite become aligned with their long spacing direction parallel to the deformation direction.²¹ In the draw region with almost constant load, the neck propagates through the sample and transforms the unoriented spherulitic into the oriented microfibrillar structure. The fourth region, with the more rapid increase of stress with extension, corresponds to plastic deformation of microfibrillar structure until the break occurs. It can be seen from Fig. 10 that as-spun multifilament yarn made from the plastic-grade polymer reaches higher stresses in the entire deformation range than as-spun multifilament yarn made from the fiber-grade polymer, which is a consequence of the more crystalline structure.

4. Conclusions

The differences in the molecular weight and molecular weight distribution of polymers resulted in different flow intensity, elongational viscosity, and consequently in the different linear density of filaments spun from the plastic-grade and fiber-grade polymer.

Despite intense air-quenching of extruded filaments, the paracrystalline, so-called smectic structure which is normally found in quickly cooled filaments was not present in our samples. In both of the as-spun multifilament yarns, the spherulitic structure with only α -monoclinic crystalline form was present. The higher molecular weight and broader molecular weight distribution of plastic-grade polymer, leading to the formation of more dense and more crystalline structure in the as-spun filaments, resulted in higher tenacity of these filaments.

5. Acknowledgements

The author wishes to acknowledge the funding support of the Ministry of Higher Education, Science and Technology.

Povzetek

Cilj raziskave je bil optimiranje talilno predilnega postopka izdelave filamentov oblikovanih iz polipropilenskega polimera nizkega talilnega indeksa. Narejena je bila primerjava strukturnih karakteristik neraztezanih filamentov, oblikovanih iz dveh različnih polimerov, polimera primerneza za izdelavo pihanih izdelkov in polimera primerneza za izdelavo vlaken. Talilno pređenje filamentov je potekalo na laboratorijski predilno-raztezalni napravi Extrusion Systems Ltd. Proces izdelave filamentov je potekal kot gravitacijsko pređenje brez faze navijanja in je bil optimiran tako, da ni prihajalo do nastanka nestabilnosti v predilni liniji in do nihanja debeline filamentov. Iz meritev molekulske mase in porazdelitve molekulskih mas je razvidno, da prihaja pri talilnem pređenju filamentov, oblikovanih iz različnih polimerov do delne degradacije molekul in zoženja porazdelitve molekulskih mas. Pri obeh, hitro hlajenih, talilno pređenih filamentih, oblikovanih iz različnih polimerov, prihaja do nastanka samo α -monoklinske sferolitne strukture. Filamenti oblikovani iz polimera primerneza za izdelavo pihanih izdelkov imajo v primerjavi s filamentmi oblikovanimi iz polimera primerneza za izdelavo vlaken višjo gostoto, talilno entalpijo in stopnjo kristalnosti, in posledično višjo trdnost.

6. References

- 1 F. J. Padden, H. D. Keith, *J. Appl. Phys.* **1959**, *30*, 1479–1485.
- 2 H. D. Keith, F. J. Padden, R. G. Vadimsky, *J. Polym. Sci., Polym. Phys.* **1966**, *4*, 267–281.
- 3 R. J. Samuels, *J. Polym. Sci., Part C* **1967**, *20*, 253–284.
- 4 A. Keller, M. J. Machin, *J. Macromol. Sci., Phys.* **1967**, *B1*, 41–91.
- 5 J. H. Southern, R. S. Porter, *J. Appl. Polym. Sci.* **1970**, *14*, 2305–2317.
- 6 K. Katayama, T. Amano, K. Nakamura, *Kolloid & Polym. Sci.* **1968**, *226*, 1435–1536.
- 7 T. Kitao, S. Ohya, J. Furukawa, S. Yamashita, *J. Polym. Sci., Polym. Phys.* **1973**, *11*, 1091–1109.
- 8 J. Shimizu, K. Shimazaki, *Sen'I Gakkaishi*, **1976**, *32*, T248.
- 9 E. Andreassen, O. J. Myhre, E. L. Hinrichsen, K. Grøstad, *J. Appl. Polym. Sci.* **1994**, *52*, 505–517.
- 10 P. Parrini, *Makromolekulare Chemie* **1963**, *62*, 83–96.
- 11 M. Ahmed, Textile Science and Technology. Vol. 5: Polypropylene Fibers – Science and Technology. Elsevier Scientific Publishing Co., Amsterdam, **1982**.
- 12 M. Compostella, A. Coen, F. Bertinotti, *Angew. Chem.* **1962**, *74*, 618–624.
- 13 S. Misra, J. E. Spruiell, G. C. Richeson, *J. of Appl. Polym. Sci.* **1995**, *56*, 1761–1779.
- 14 C. D. Han, *J. Appl. Polym. Sci.* **1971**, *15*, 1149–1162.
- 15 C. D. Han, *J. Appl. Polym. Sci.* **1971**, *15*, 2567–2577.
- 16 R. Janarthanan, S. N. Garg, A. Misra, *J. Appl. Polym. Sci.* **1994**, *51*, 1175–1182.
- 17 H. P. Nadella, H. M. Henson, J. E. Spruiell, J. W. White, *J. Appl. Polym. Sci.* **1977**, *21*, 3003–3022.
- 18 F. Lu, J. E. Spruiell, *J. of Appl. Polym. Sci.* **1987**, *34*, 1521–1539.
- 19 H. P. Klug, L. E. Alexander, X-ray Diffraction Procedures, Wiley, New York, **1973**.
- 20 A. Weidinger, P. H. Hermans, *Makromol. Chem.* **1961**, *50*, 98–115.
- 21 R. J. Samuels, *J. Macromol. Sci.-Phys.* **1970**, *B4(3)*, 701–759.